

Hydrothermal synthesis of Cr and Fe co-doped TiO₂ nanoparticle photocatalyst

E.D. Jeong^a, Pramod H. Borse^b, J.S. Jang^b, J.S. Lee^b, Ok-Sang Jung^c, H. Chang^d, J.S. Jin^a, M.S. Won^a and H.G. Kim^{a,*}

^aBusan Center, Korea Basic Science Institute, Busan 609-735, Korea

^bDepartment of Chemical Engineering, Pohang University of Science and Technology, Pohang 790-784, Korea

^cDepartment of Chemistry(BK21), Pusan National University, Pusan 609-735, Korea

^dKorea Research Institute of Chemical Technology, Daejeon 305-600, Korea

We report here new findings on the visible light photodecomposition activity of gaseous iso-propyl alcohol over Cr and Fe co-doped TiO₂ nanoparticles. High surface area, doped TiO₂ nanoparticles were synthesized hydrothermally and co-dopant effects are investigated. The physico-chemical properties of the co-doped nanoparticles led to efficient photocatalysts. Cr and Fe co-doped TiO₂ nanoparticles exhibited two times higher photocatalytic activity for the photodecomposition of gaseous isopropyl alcohol than the individually (Cr/Fe) doped TiO₂ nanoparticles under visible light irradiation ($\lambda > 420$ nm). The activity is mainly correlated to the larger absorptions around 496nm and 563nm wavelengths by co-doped TiO₂ nanoparticles than Fe doped TiO₂ nanoparticles which possibly absorb $\lambda > 496$ nm.

Key words: Cr and Fe co-doped TiO₂, Nano-particles, Hydrothermal synthesis method, Photocatalysts.

Introduction

Photon-induced chemical conversion using solar radiation, has been a main focus of research since 1972 when Honda and Fujishima [1] first reported the photocatalytic ability of TiO₂ to generate oxygen and hydrogen by splitting water. The photo-induced chemical conversion is of great importance for an efficient pollution abatement and energy conversion. Titanium dioxide, an inexpensive metal oxide semiconductor has demonstrated high activity and stability for its applications in organic and inorganic pollutant degradation to purify air and water [2-5] and in obtaining superhydrophilicity of the solid surfaces. [6, 7] However, TiO₂ is active only under ultraviolet (UV) light ($\lambda < 400$ nm) due to its wide band gap of ca. 3.2 eV (for the crystalline anatase phase). Since the fraction of UV radiation in the solar spectrum is less than 5%, [8] TiO₂ cannot exploit efficiently the abundant solar radiation (dominant visible light) on earth. For a smarter utilization of this dominant part of the solar spectrum as well as indoor applications under weak interior lighting, the photocatalyst must be able to absorb visible light photons. Consequently, the search of visible light-active photocatalysts has become a subject of intense research even today.

Apart from traditional visible-light photocatalysts (CdS, WO₃, Fe₂O₃, etc), [9, 10] two main popular paths have been followed in this search; (i) to hunt for new

materials with suitable visible-light activity[11, 14] and (ii) to modify the electronic structure of the known UV active photocatalysts by intentional doping or substitution. For the second case, the trend has been to convert the UV-active oxides by cationic doping, as in Ni_xIn_{1-x}TaO₄ and (V-, Fe-, or Mn-) TiO₂ or SrTiO₃, [15, 18] or anionic doping of C, N and S, as in TiO_{2-x}N_x, and TiO_{2-x}C_x [19-21]. However, these original lattices could accommodate only very small dopant levels (much less than 10 atomic%) without destroying the original structure. Thus, in general, doped materials show a small absorption in the visible light region with the original band gap absorption in the UV region intact, rather than a total red-shift of the band gap energy [22]. This limitation has contributed to their low activities. The nanoparticle photocatalyst form a different category of photocatalysts, which do need independent attention.

Here, we report the new findings on Cr and Fe co-doped TiO₂ nanoparticles prepared by a hydrothermal synthesis method, which showed a high activity for the photo degradation of organic compounds under visible light irradiation ($\lambda > 420$ nm). We studied the optical structure of doped TiO₂ nanoparticles and correlated the physico-chemical properties with their photocatalytic behavior.

Experimental

Cr and Fe co-doped TiO₂ nanoparticles were made by a hydrothermal treatment (HT). The procedure involved preparation of a sol and its hydrothermal treatment. Accordingly, TiO₂ sol was prepared from a controlled sol-gel method using titanium isopropoxide Ti(OCH(CH₃)₂)₄ (99.0%, Aldrich Co.). One molar solution of Ti(OCH(CH₃)₂)₄

*Corresponding author:
Tel : +82-51-510-1903
Fax: +82-51-517-2497
E-mail: hhgkim@kbsi.re.kr

in absolute ethanol (5 ml) was drop-wise added to 47 ml of distilled water under vigorous stirring. The final pH was adjusted to 1.77 with nitric acid. Then 0.1 molar solutions of Fe(NO₃)₃·6H₂O and Cr(NO₃)₃·6H₂O were dissolved in distilled water. The TiO₂ sol was drop-wise added to the aqueous solutions of Fe(NO₃)₃·6H₂O/Cr(NO₃)₃·6H₂O in a water bath with continuous stirring. The final mixture was stirred for 2 h at 50 °C until it became a transparent greenish clear solution for Cr and Fe co-doped TiO₂. The mixture finally obtained was subjected to a hydrothermal treatment for 5 days at 180 °C and were further calcined at 400 °C for 5 h in an electric furnace to obtain crystalline powders of TiO₂. For the purpose of comparison, nitrogen-doped TiO₂ was prepared by the hydrolytic synthesis (HS) method, in which an ammonium hydroxide aqueous solution with an ammonia content of 28-30% (99.99%, Aldrich Co.) was slowly added drop-by-drop to titanium (III) chloride (TiCl₃, 99.0%, Aldrich Co.) under a N₂ flow in an ice bath while continuously stirred. These samples were further calcined at 400 °C for 2 h in an electric furnace to obtain crystalline powders of TiO_{2-x}N_x. The bulk-type TiO₂ was prepared from the controlled sol-gel method of Ti(OCH(CH₃)₂)₄.

The Cr and Fe co-doped TiO₂ crystalline powders were characterized by high-resolution transmission electron microscopy (HR-TEM, Phillips Model CM 200), UV-vis diffuse reflectance spectroscopy (Shimadzu, UV 2401), powder X-ray diffraction (XRD, Mac Science Co., M18XHF). The BET surface area of Cr and Fe co-doped TiO₂ were evaluated by N₂ adsorption on a constant volume adsorption apparatus (Micrometrics, ASAP2012). About 200 ppm of gaseous isopropyl alcohol (IPA) was injected into a 500-ml Pyrex reaction cell filled with air and containing 0.3 g of a catalyst. The concentration of the reaction products (CO₂) was determined by a gas chromatograph equipped with a thermal conductivity detector and a molecular sieve 5-Å column.

Results

Figure 1 displays the XRD patterns of pure and doped anatase TiO₂ nanoparticles. All the samples exhibited the anatase structure of TiO₂. The lattice parameter of anatase TiO₂ with a tetragonal crystal structure was estimated to be $a = b = 3.78 \text{ \AA}$ and $c = 9.49 \text{ \AA}$. There was no effect of the dopants on the crystal structure with the dopant concentration used in the present study. The doped TiO₂ did not show the presence of chromium or iron related oxide phases.

The crystallite size (D) can be calculated using the Scherrer's equation,²³ $D = 0.9\lambda/B \cos \theta$, where λ is the wavelength of X-ray radiation ($\lambda = 0.154 \text{ nm}$), B is FWHM of the peak (radians) corrected for instrumental broadening, θ is Bragg angle, and D is the particle size (nm). The average particle size for TiO₂ samples used in the study was found to be 18 nm.

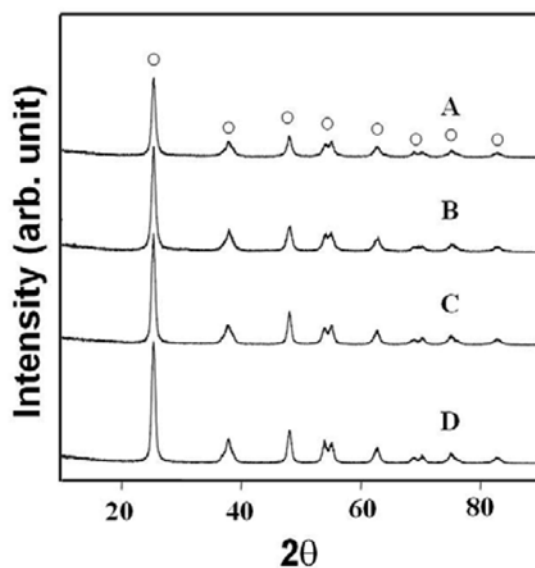


Fig. 1. Powder XRD patterns of various materials (A) Cr-doped TiO₂, (B) Fe-doped TiO₂, (C) Fe and Cr co-doped TiO₂, (D) TiO₂ calcined at 400 °C. O : Anatase phase.

Figure 2 shows HR-TEM images of the samples (A; Cr and Fe co-doped TiO₂, B; TiO_{2-x}N_x) calcined at 400 °C. Figure 2(A) indicates that the average particle size of Cr and Fe co-doped TiO₂ particles at 21 nm, in near agreement with the sizes estimated from XRD (*ca.* 18 nm). The particle sizes for M-doped TiO₂ (M = Cr or Fe) particles were also found to be similar as for the co-doped TiO₂ particles. The TiO_{2-x}N_x samples however consisted of fine particles yielding agglomerates of around 200 nm. The particle sizes of metal doped TiO₂ prepared by the HT method were smaller than TiO_{2-x}N_x particles obtained by the HS method.

The optical properties of pure and doped TiO₂ were probed by UV-DRS as shown in Fig. 3 which shows that co-doped TiO₂ exhibit larger absorption in the visible light region than others doped or pure TiO₂. The main absorption edge of TiO₂ was estimated to be about 387 nm

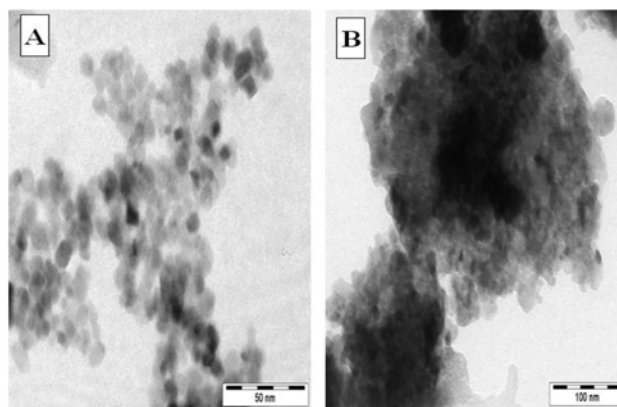


Fig. 2. TEM images of samples (A) Fe and Cr co-doped TiO₂, (B) N-doped TiO₂ calcined at 400 °C.

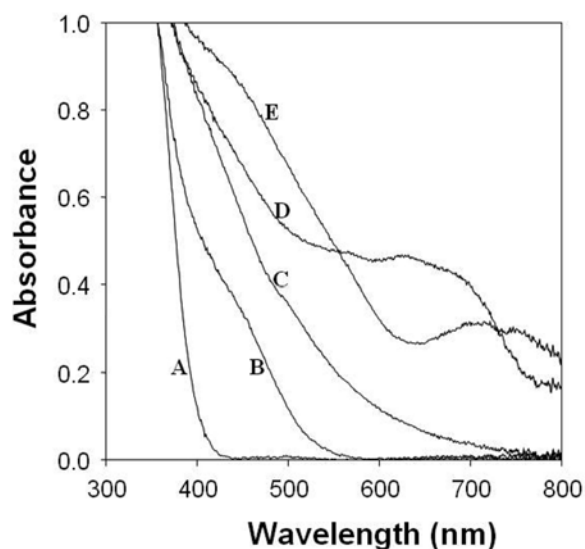


Fig. 3. UV-vis diffuse reflectance spectra for the various materials. A, TiO₂; B, TiO_{2-x}N_x; C, Fe-doped TiO₂; D, Cr and Fe co-doped TiO₂; E, Cr-doped TiO₂.

(3.2 eV). However, doped TiO₂ (M = Cr and Fe), Cr and Fe metals co-doped TiO₂ and TiO_{2-x}N_x showed shoulder peaks in the wavelength range of 450-700 nm, which were absent in the spectrum of TiO₂. It is reported that Cr³⁺ and Fe³⁺ ions show strong absorption bands in the UV region[24]. Therefore, these shoulder peaks are probably due to the absorption induced due to dopants. The energy gaps estimated from the UV-vis spectra of doped TiO₂ and Cr and Fe co-doped TiO₂ are in the visible light region of 1.8-2.31 eV. These band gap energies are greater than the theoretical energy required for splitting water (> 1.23 eV). Table 1 summarizes results of the physical characterization of different materials under study. Further, the BET surface areas of Cr and Fe metals co-doped TiO₂ is similar to Fe/Cr doped TiO₂, but higher than TiO_{2-x}N_x and TiO₂.

To evaluate the photocatalytic activities of these materials under visible light ($\lambda > 420$ nm), oxidative decomposition of gaseous IPA was carried out. Figure 4 shows the time courses of CO₂ evolution from IPA decomposition

Table 1. Band gap energy and BET surface areas of various materials

Photocatalyst	Calcination temperature (°C)	BET surface area (m ² /g)	Band gap(a) energy (eV)
Cr-Fe co-doped TiO ₂	400	93	2.52
Cr-doped TiO ₂	400	86	2.31
Fe-doped TiO ₂	400	89	2.51
TiO _{2-x} N _x	400	48	2.73
TiO ₂	-	51	3.20

(a) The wavelength at the absorption edge, λ , was determined as the intercept on the wavelength axis for a tangent line drawn on absorption spectra.

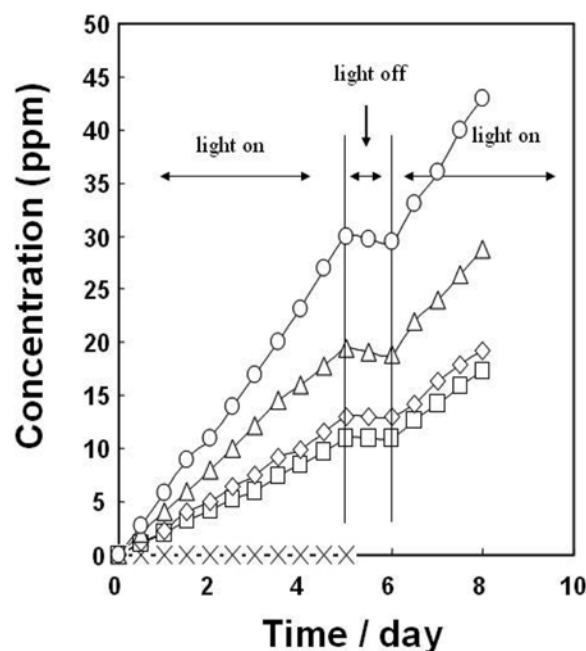


Fig. 4. Time courses of CO₂ evolution from IPA decomposition over various materials under visible light irradiation ($\lambda \geq 420$ nm). Material, 0.3 g; IPA concentration, 200 ppm in air. X, TiO₂; □, Cr-doped TiO₂; ◇, TiO_{2-x}N_x; △, Fe-doped TiO₂; ○, Cr and Fe co-doped TiO₂.

over various materials as a function of irradiation time. TiO₂ showed no photocatalytic activity for IPA degradation to CO₂ under visible light. However, doped and pure TiO₂ showed the activity for IPA degradation to CO₂. Interestingly, Cr-Fe co-doped TiO₂ showed the highest activity. In the case of TiO_{2-x}N_x and doped TiO₂, the concentration of CO₂ increased rapidly with increasing irradiation time. The photocatalytic activity of Cr-doped TiO₂ for IPA degradation was similar to that for TiO_{2-x}N_x. The CO₂ production stopped when the light was turned off and was resumed at the same rate when light was turned on again. The Cr and Fe co-doped TiO₂ showed much higher decomposition rates and activities than those of Cr/Fe doped TiO₂ for IPA degradation. Thus, the material co-doped with Cr and Fe exhibited two times higher photocatalytic activity for photodecomposition of IPA gases than Cr/Fe doped particles under visible light.

Discussion

The favorable effect of co-dopants on the photocatalytic performance was further analyzed. It can be recalled that the TiO₂ band gap consists of a contribution from O 2p orbitals for the valence band and from Ti 4d orbitals towards the conduction band. The band structures of the Fe/Cr doped and co-doped TiO₂ are mainly affected by the 3d bands/energy states of these transition metal ions (Cr³⁺ and Fe³⁺), thus the UV-vis absorption studies do also indicate the respective absorptions below the main

absorption edges of TiO₂ as described in the above section. Thus, it also possibly indicates that the partially filled Fe/Cr 3d band are located 2.2-2.5 eV below the conduction band. Hence, when photons with wavelengths longer than 420 nm are used for illumination, the electrons in the Cr 3d and Fe 3d interbands, instead of electrons in the valence band of TiO₂, are excited to the conduction band, while Cr³⁺ and Fe³⁺ loses one electron and becomes Cr⁴⁺ and Fe⁴⁺. There is no such photo-excitation of electrons in the valence band of TiO₂ because the energy of the incident light is much less than the band gap energy. Thus, Cr and Fe metals co-doped TiO₂ absorb more visible light photons than those of Fe/Cr doped TiO₂. The band gap energy for Cr and Fe co-doped TiO₂ indicates that the minimum energy photons necessary to produce conduction band electrons, which, for example, can give rise to valence band "holes", which are actually the absence of electrons [25]. These holes can react with water to produce the highly reactive ·OH. Both the holes and the ·OH have a strong oxidation potential for the degradation of organic compounds. Thus above discussion indicates a guideline to understand the role of Cr- and Fe- co-doped TiO₂ nanoparticles in yielding better performance as a visible light photocatalyst.

Conclusions

In order to develop efficient photocatalysts working with sun light, transition metals co-doped TiO₂ nanoparticles were synthesized by the hydrothermal synthesis method and their co-doping effect was analyzed on the photodecomposition of IPS. The average diameter of the Cr and Fe metals co-doped TiO₂ particles was estimated to be 21 nm. They exhibited two times higher photocatalytic activity for photodecomposition of gaseous isopropyl alcohol (IPA) than did the individually (Cr/Fe) doped TiO₂ nanoparticles under visible light irradiation ($\lambda > 420$ nm). The activity is mainly correlated to the larger absorptions around 496 nm and 563 nm wavelengths by co-doped TiO₂ nanoparticles than Fe doped TiO₂ nanoparticles which possibly absorb $\lambda \leq 496$ nm.

Acknowledgement

This work has been supported by KBSI grant (No. N28035), KOSEF grant (NCRCP, No. R15-2006-022-01002-0) and Hydrogen Energy R&D Center, Korea.

References

1. A. Fujishima and K. Honda, *Nature* 238 (1972) 37.
2. M.R. Hoffman, S.T. Martin, W. Choi and D.W. Bahnemann, *Chem. Rev.* 95 (1995) 69.
3. N. Serpone and E. Pelizzetti, in *Photocatalysis Fundamental and applications*, John Wiley & Sons, New York (1989) p. 607.
4. B.W. Lee, H. Cho and D.W. Shin, *J. Ceram. Pro. Res.* 8 (2007) 203.
5. J.H. An, B.H. Kim, J.H. Jeong, D.M. Kim, Y.S. Jeon, K.O. Jeon and K. S. Hwang, *J. Ceram. Pro. Res.* 6 (2005) 163.
6. R. Wang, K. Hashimoto, A. Fujishima, M. Chikuni, E. Kojima, A. Kitamura, M. Shimohigoshi and T. Watanabe, *Nature* 388 (1997) 431.
7. H.C. Kim, H.K. Park, I.J. Shon and I.Y. Ko, *J. Ceram. Pro. Res.* 7 (2006) 327.
8. G.C. Granqvist, *Adv. Mater.* 15 (2003) 1789.
9. G.C. De, A.M. Roy and S.S. Bhattacharya, *Int. J. Hydrogen Energy* 21(1996) 19.
10. D.W. Hwang, J. Kim, T.J. Park and J.S. Lee, *Catal. Lett.* 80 (2002) 53.
11. H.G. Kim, D.W. Hwang and J.S. Lee, *J. Am. Chem. Soc.* 126 (2004) 8912.
12. J. Tang, Z. Zou and J. Ye, *Angew. Chem. Int. Ed.* 43 (2004) 4463.
13. G. Hitoki, T. Takata, J.N. Kondo, M. Hara, H. Kobayashi and K. Domen, *Chem. Commun.* 1698 (2002).
14. A. Ishikawa, T. Takata, J.N. Kondo, M. Hara, H. Kobayashi and K. Domen, *J. Am. Chem. Soc.* 124 (2002) 13547.
15. Z. Zou, J. Ye, K. Sayama and H. Arakawa, *Nature* 424 (2001) 625.
16. H. Yamashita, H. Harada, J. Misaka, M. Takeuchi, K. Ikeue and M. Anpo, *Photochem. Photobiol. A* 148 (2002) 257.
17. K. Kato and A. Kudo, *J. Phys. Chem. B* 106 (2002) 5029.
18. D.W. Hwang, H.G. Kim, J.S. Lee, W. Li and S.H. Oh, *J. Phys. Chem. B* 109 (2005) 2093.
19. R. Asahi, T. Morikawa, T. Ohwaki, K. Aoki and Y. Taga, *Science* 293 (2001) 269.
20. S.U.M. Khan, M. Al-Shahry and W.B. Jr. Ingler, *Science* 297 (2002) 2243.
21. S. Sakthivel and H. Kisch, *Angew. Chem. Int. Ed.* 42 (2003) 4908.
22. D.W. Hwang, H.G. Kim, J.S. Jang, S.W. Bae, S.M. Ji and J.S. Lee, *Catal. Today* 93-95 (2004) 845.
23. B.D. Cullity, 2nd Edition, Addison-Wesley Publishing Company, Inc., Reading, MA (1978).
24. B. Henderson and G.F. Imbusch, in *Optical Spectroscopy of Inorganic Solids*, Clarendon Press, Oxford (1989).
25. A. Fujishima, K. Hashimoto and T. Watanabe, in *TiO₂ Photocatalysis: Fundamentals and Applications*, BKC Inc., Tokyo (1999).